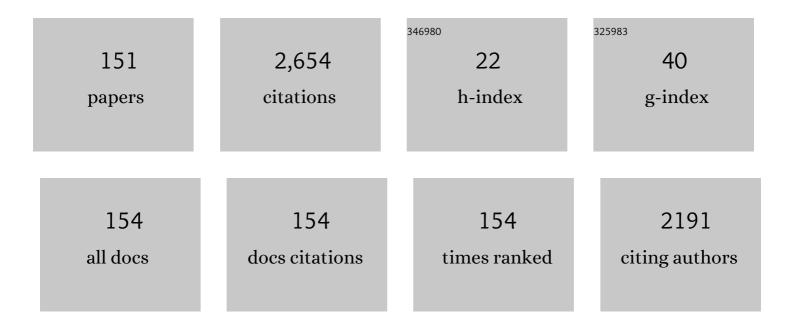
List of Publications by Year in descending order

Source: https://exaly.com/author-pdf/1044347/publications.pdf Version: 2024-02-01



RVO ASAOKA

#	Article	IF	CITATIONS
1	Faster algorithms to measure visual field using the variational Bayes linear regression model in glaucoma: comparison with SITA-Fast. British Journal of Ophthalmology, 2023, 107, 946-952.	2.1	2
2	Comparing the usefulness of a new algorithm to measure visual field using the variational Bayes linear regression in glaucoma patients, in comparison to the Swedish interactive thresholding algorithm. British Journal of Ophthalmology, 2022, 106, 660-666.	2.1	5
3	Validating the usefulness of sectorwise regression of visual field in the central 10°. British Journal of Ophthalmology, 2022, 106, 497-501.	2.1	2
4	Deep learning-assisted (automatic) diagnosis of glaucoma using a smartphone. British Journal of Ophthalmology, 2022, 106, 587-592.	2.1	13
5	Relationship between the vessel density around the optic nerve head and visual field deterioration in eyes with retinitis pigmentosa. Graefe's Archive for Clinical and Experimental Ophthalmology, 2022, 260, 1097-1103.	1.0	4
6	Foveal microstructure and visual function in patients with lamellar macular hole, epiretinal membrane foveoschisis or macular pseudohole. Eye, 2022, 36, 2247-2252.	1.1	2
7	Relationships between Skin Carotenoid Levels and Metabolic Syndrome. Antioxidants, 2022, 11, 14.	2.2	9
8	Case Report: Microincision Vitreous Surgery Induces Bleb Failure in Eyes With Functional Filtering Bleb. Frontiers in Medicine, 2022, 9, 847660.	1.2	0
9	Comparison of surgical outcomes between initial trabeculectomy and Ex-PRESS in terms of achieving an intraocular pressure below 15 and 18ÂmmHg: a retrospective comparative study. Eye and Vision (London, England), 2022, 9, 9.	1.4	2
10	Relationship between visual acuity and visual field and its reproducibility in patients with retinitis pigmentosa. Eye, 2022, , .	1.1	0
11	Binocular superior visual field areas associated with driving self-regulation in patients with primary open-angle glaucoma. British Journal of Ophthalmology, 2021, 105, 135-140.	2.1	2
12	Deep learning model to predict visual field in central 10º from optical coherence tomography measurement in glaucoma. British Journal of Ophthalmology, 2021, 105, 507-513.	2.1	32
13	Does the number of laser applications for ROP treatment influence the degree of myopia?. Graefe's Archive for Clinical and Experimental Ophthalmology, 2021, 259, 317-322.	1.0	6
14	Aqueous autotaxin and TGF-βs are promising diagnostic biomarkers for distinguishing open-angle glaucoma subtypes. Scientific Reports, 2021, 11, 1408.	1.6	21
15	Prevalence of Epiretinal Membrane among Subjects in a Health Examination Program in Japan. Life, 2021, 11, 93.	1.1	1
16	Quantification of residual ellipsoid zone and its correlation with visual functions in patients with cone-rod dystrophy. European Journal of Ophthalmology, 2021, 31, 3117-3123.	0.7	6
17	Improving Visual Field Trend Analysis with OCT and Deeply Regularized Latent-Space Linear Regression. Ophthalmology Glaucoma, 2021, 4, 78-88.	0.9	3
18	Correlation between fundus autofluorescence and visual function in patients with cone-rod dystrophy. Scientific Reports, 2021, 11, 1911.	1.6	3

#	Article	lF	CITATIONS
19	Visual outcomes and prognostic factors of vitrectomy for lamellar macular holes and epiretinal membrane foveoschisis. PLoS ONE, 2021, 16, e0247509.	1.1	8
20	Correction for the Influence of Cataract on Macular Pigment Measurement by Autofluorescence Technique Using Deep Learning. Translational Vision Science and Technology, 2021, 10, 18.	1.1	5
21	Assessment of the choroidal structure in pregnant women in the first trimester. Scientific Reports, 2021, 11, 4629.	1.6	7
22	Long-Term Follow-Up After Successful Trabeculectomy: A Case Report of Reversal of Cupping and Recovery of Visual Field Progression. Cureus, 2021, 13, e13520.	0.2	0
23	Predicting intraocular pressure using systemic variables or fundus photography with deep learning in a health examination cohort. Scientific Reports, 2021, 11, 3687.	1.6	7
24	Macular pigment changes after cataract surgery with yellow-tinted intraocular lens implantation. PLoS ONE, 2021, 16, e0248506.	1.1	1
25	Association of Near-Infrared and Short-Wavelength Autofluorescence With the Retinal Sensitivity in Eyes With Resolved Central Serous Chorioretinopathy. , 2021, 62, 36.		6
26	Macular irregularities of optical coherence tomographic vertical cross sectional images in school age children. Scientific Reports, 2021, 11, 5284.	1.6	1
27	Investigating the clinical usefulness of definitions of progression with 10-2 visual field. British Journal of Ophthalmology, 2021, , bjophthalmol-2020-318188.	2.1	2
28	Correlation between choroidal structure and smoking in eyes with central serous chorioretinopathy. PLoS ONE, 2021, 16, e0249073.	1.1	5
29	Retinal vessel shift and its association with axial length elongation in a prospective observation in Japanese junior high school students. PLoS ONE, 2021, 16, e0250233.	1.1	2
30	Relationship Between Optical Coherence Tomography Parameter and Visual Function in Eyes With Epiretinal Membrane. , 2021, 62, 6.		8
31	Development and validation of a visual field cluster in retinitis pigmentosa. Scientific Reports, 2021, 11, 9671.	1.6	3
32	Biomechanical Glaucoma Factor and Corneal Hysteresis in Treated Primary Open-Angle Glaucoma and Their Associations With Visual Field Progression. , 2021, 62, 4.		12
33	Evaluation of rebound tonometer iCare IC200 as compared with IcarePRO and Goldmann applanation tonometer in patients with glaucoma. Eye and Vision (London, England), 2021, 8, 25.	1.4	10
34	Assessment of macular function in patients with non-vascularized pigment epithelial detachment. Scientific Reports, 2021, 11, 16577.	1.6	1
35	The Relationship Between Optic Disc and Retinal Artery Position and Glaucomatous Visual Field Progression. , 2021, 62, 6.		1
36	A Joint Multitask Learning Model for Cross-sectional and Longitudinal Predictions of Visual Field Using OCT. Ophthalmology Science, 2021, 1, 100055.	1.0	7

#	Article	IF	CITATIONS
37	Predicting the central 10 degrees visual field in glaucoma by applying a deep learning algorithm to optical coherence tomography images. Scientific Reports, 2021, 11, 2214.	1.6	27
38	Sex Differences in Rate of Axial Elongation and OcularÂBiometrics in Elementary School Students. Clinical Ophthalmology, 2021, Volume 15, 4297-4302.	0.9	2
39	Association between serum soluble fms-like tyrosine kinase-1 and the central choroidal thickness during pregnancy: a prospective study. BMJ Open Ophthalmology, 2021, 6, e000888.	0.8	0
40	Association between the number of visual fields and the accuracy of future prediction in eyes with retinitis pigmentosa. BMJ Open Ophthalmology, 2021, 6, e000900.	0.8	0
41	Predicting 10-2 Visual Field From Optical Coherence Tomography in Glaucoma Using Deep Learning Corrected With 24-2/30-2 Visual Field. Translational Vision Science and Technology, 2021, 10, 28.	1.1	10
42	Lutein and Zeaxanthin Distribution in the Healthy Macula and Its Association with Various Demographic Factors Examined in Pseudophakic Eyes. Antioxidants, 2021, 10, 1857.	2.2	6
43	Using ultra-widefield red channel images to improve the detection of ischemic central retinal vein occlusion. PLoS ONE, 2021, 16, e0260383.	1.1	2
44	Detecting Progression of Retinitis Pigmentosa Using the Binomial Pointwise Linear Regression Method. Translational Vision Science and Technology, 2021, 10, 15.	1.1	2
45	Real-World Analysis of the Aging Effects on Visual Field Reliability Indices in Humans. Journal of Clinical Medicine, 2021, 10, 5775.	1.0	3
46	Predicting Humphrey 10-2 visual field from 24-2 visual field in eyes with advanced glaucoma. British Journal of Ophthalmology, 2020, 104, 642-647.	2.1	11
47	Relationship between novel intraocular pressure measurement from Corvis ST and central corneal thickness and corneal hysteresis. British Journal of Ophthalmology, 2020, 104, 563-568.	2.1	19
48	Validating the efficacy of the binomial pointwise linear regression method to detect glaucoma progression with multicentral database. British Journal of Ophthalmology, 2020, 104, 569-574.	2.1	6
49	Comment on Cataract Surgery and Rate of Visual Field Progression in Primary Open-Angle Glaucoma. American Journal of Ophthalmology, 2020, 209, 216-217.	1.7	2
50	Association between optic nerve head morphology in open-angle glaucoma and corneal biomechanical parameters measured with Corvis ST. Graefe's Archive for Clinical and Experimental Ophthalmology, 2020, 258, 629-637.	1.0	7
51	The Relationship Between Corneal Hysteresis and Progression of Glaucoma After Trabeculectomy. Journal of Glaucoma, 2020, 29, 912-917.	0.8	8
52	Short wavelength automated perimetry and standard automated perimetry in central serous chorioretinopathy. Scientific Reports, 2020, 10, 16451.	1.6	1
53	Time course of conjunctival hyperemia induced by omidenepag isopropyl ophthalmic solution 0.002%: a pilot, comparative study versus ripasudil 0.4%. BMJ Open Ophthalmology, 2020, 5, e000538.	0.8	9
54	Usefulness of data augmentation for visual field trend analyses in patients with glaucoma. British Journal of Ophthalmology, 2020, 104, 1697-1703.	2.1	3

#	Article	IF	CITATIONS
55	Bleb plication: a minimally invasive repair method for a leaking ischemic bleb after trabeculectomy. Scientific Reports, 2020, 10, 14978.	1.6	4
56	A Prediction Method of Visual Field Sensitivity Using Fundus Autofluorescence Images in Patients With Retinitis Pigmentosa. , 2020, 61, 51.		4
57	Comparison between blue-on-yellow and white-on-white perimetry in patients with branch retinal vein occlusion. Scientific Reports, 2020, 10, 20009.	1.6	1
58	Sex judgment using color fundus parameters in elementary school students. Graefe's Archive for Clinical and Experimental Ophthalmology, 2020, 258, 2781-2789.	1.0	4
59	The usefulness of the Deep Learning method of variational autoencoder to reduce measurement noise in glaucomatous visual fields. Scientific Reports, 2020, 10, 7893.	1.6	8
60	Effects of Study Population, Labeling and Training on Glaucoma Detection Using Deep Learning Algorithms. Translational Vision Science and Technology, 2020, 9, 27.	1.1	35
61	Factors in Color Fundus Photographs That Can Be Used by Humans to Determine Sex of Individuals. Translational Vision Science and Technology, 2020, 9, 4.	1.1	21
62	The usefulness of the retinal sensitivity measurement with a microperimetry for predicting the visual prognosis of branch retinal vein occlusion with macular edema. Graefe's Archive for Clinical and Experimental Ophthalmology, 2020, 258, 1949-1958.	1.0	11
63	Effect of Manual Upper Eyelid Elevation on Intraocular Pressure Measurement by Four Different Tonometers. Optometry and Vision Science, 2020, 97, 128-133.	0.6	3
64	Structural Changes and Astrocyte Response of the Lateral Geniculate Nucleus in a Ferret Model of Ocular Hypertension. International Journal of Molecular Sciences, 2020, 21, 1339.	1.8	12
65	Visualizing the dynamic change of Ocular Response Analyzer waveform using Variational Autoencoder in association with the peripapillary retinal arteries angle. Scientific Reports, 2020, 10, 6592.	1.6	3
66	Predicting the Glaucomatous Central 10-Degree Visual Field From Optical Coherence Tomography Using Deep Learning and Tensor Regression. American Journal of Ophthalmology, 2020, 218, 304-313.	1.7	19
67	Improving the Structure–Function Relationship in Glaucomatous Visual Fields by Using a Deep Learning–Based Noise Reduction Approach. Ophthalmology Glaucoma, 2020, 3, 210-217.	0.9	10
68	Factors in Color Fundus Photographs That Can Be Used by Humans to Determine Sex of Individuals. Translational Vision Science and Technology, 2020, 210, 1737.	1.1	0
69	Repeatability of the Novel Intraocular Pressure Measurement From Corvis ST. Translational Vision Science and Technology, 2019, 8, 48.	1.1	11
70	Investigating the structureâ€function relationship using Goldmann V standard automated perimetry where glaucomatous damage is advanced. Ophthalmic and Physiological Optics, 2019, 39, 441-450.	1.0	0
71	Correlation Between the Myopic Retinal Deformation and Corneal Biomechanical Characteristics Measured With the Corvis ST Tonometry. Translational Vision Science and Technology, 2019, 8, 26.	1.1	3
72	Development of a Novel Corneal Concavity Shape Parameter and Its Association with Glaucomatous Visual Field Progression. Ophthalmology Glaucoma, 2019, 2, 47-54.	0.9	5

#	Article	IF	CITATIONS
73	Retinal sensitivity in angioid streaks. Graefe's Archive for Clinical and Experimental Ophthalmology, 2019, 257, 1591-1599.	1.0	1
74	Relationship Between the Shift of the Retinal Artery Associated With Myopia and Ocular Response Analyzer Waveform Parameters. Translational Vision Science and Technology, 2019, 8, 15.	1.1	5
75	Relationship between the Vertical Asymmetry of the Posterior Pole of the Eye and the Visual Field Damage in Glaucomatous Eyes. Ophthalmology Glaucoma, 2019, 2, 28-35.	0.9	2
76	The association of choroidal structure and its response to anti-VEGF treatment with the short-time outcome in pachychoroid neovasculopathy. PLoS ONE, 2019, 14, e0212055.	1.1	21
77	Estimating the Reliability of Glaucomatous Visual Field for the Accurate Assessment of Progression Using the Gaze-Tracking and Reliability Indices. Ophthalmology Glaucoma, 2019, 2, 111-119.	0.9	11
78	Outcomes of Wider Area Bleb Revision Using Bleb Knife With Adjunctive Mitomycin C. Journal of Glaucoma, 2019, 28, 732-736.	0.8	2
79	Comparison of the Intraocular Pressure Measured Using the New Rebound Tonometer Icare ic100 and Icare TA01i or Goldmann Applanation Tonometer. Journal of Glaucoma, 2019, 28, 172-177.	0.8	19
80	Early Detection of Glaucomatous Visual Field Progression Using Pointwise Linear Regression With Binomial Test in the Central 10 Degrees. American Journal of Ophthalmology, 2019, 199, 140-149.	1.7	12
81	Using Deep Learning and Transfer Learning to Accurately Diagnose Early-Onset Glaucoma From Macular Optical Coherence Tomography Images. American Journal of Ophthalmology, 2019, 198, 136-145.	1.7	164
82	Validation of a Deep Learning Model to Screen for Glaucoma Using Images from Different Fundus Cameras and Data Augmentation. Ophthalmology Glaucoma, 2019, 2, 224-231.	0.9	42
83	Detecting glaucomatous progression with infrequent visual field testing. Ophthalmic and Physiological Optics, 2018, 38, 174-182.	1.0	6
84	The effect of air pulse-driven whole eye motion on the association between corneal hysteresis and glaucomatous visual field progression. Scientific Reports, 2018, 8, 2969.	1.6	12
85	Evaluating the Usefulness of MP-3 Microperimetry in Glaucoma Patients. American Journal of Ophthalmology, 2018, 187, 1-9.	1.7	39
86	The association between ocular surface measurements with visual field reliability indices and gaze tracking results in preperimetric glaucoma. British Journal of Ophthalmology, 2018, 102, 525-530.	2.1	4
87	The Relationship between the Waveform Parameters from the Ocular Response Analyzer and the Progression of Glaucoma. Ophthalmology Glaucoma, 2018, 1, 123-131.	0.9	7
88	Rates of Visual Field Loss in Primary Open-Angle Glaucoma and Primary Angle-Closure Glaucoma: Asymmetric Patterns. , 2018, 59, 5717.		15
89	Correlation between elastic energy stored in an eye and visual field progression in glaucoma. PLoS ONE, 2018, 13, e0204451.	1.1	7
90	Development of a deep residual learning algorithm to screen for glaucoma from fundus photography. Scientific Reports, 2018, 8, 14665.	1.6	177

#	Article	IF	CITATIONS
91	Two-year outcome of treat-and-extend aflibercept after ranibizumab in age-related macular degeneration and polypoidal choroidal vasculopathy patients. Clinical Ophthalmology, 2018, Volume 12, 1589-1597.	0.9	7
92	Asymmetric Patterns of Visual Field Defect in Primary Open-Angle and Primary Angle-Closure Glaucoma. , 2018, 59, 1279.		31
93	Investigating the Usefulness of Fundus Autofluorescence in Retinitis Pigmentosa. Ophthalmology Retina, 2018, 2, 1062-1070.	1.2	10
94	Corneal biomechanical properties are associated with the activity and prognosis of Angioid Streaks. Scientific Reports, 2018, 8, 8130.	1.6	7
95	Changes in Axial Length and Progression of Visual Field Damage in Glaucoma. , 2018, 59, 407.		17
96	Mapping the Central 10° Visual Field to the Optic Nerve Head Using the Structure–Function Relationship. , 2018, 59, 2801.		9
97	Changes in Corneal Biomechanics and Intraocular Pressure Following Cataract Surgery. American Journal of Ophthalmology, 2018, 195, 26-35.	1.7	34
98	Improving the structure-function relationship in glaucomatous and normative eyes by incorporating photoreceptor layer thickness. Scientific Reports, 2018, 8, 10450.	1.6	8
99	Choroidal structure as a biomarker for visual acuity in intravitreal aflibercept therapy for polypoidal choroidal vasculopathy. PLoS ONE, 2018, 13, e0197042.	1.1	6
100	Factors associated with developing a fear of falling in subjects with primary open-angle glaucoma. BMC Ophthalmology, 2018, 18, 39.	0.6	11
101	Estimating Claucomatous Visual Sensitivity from Retinal Thickness with Pattern-Based Regularization and Visualization. , 2018, , .		15
102	Validating Variational Bayes Linear Regression Method With Multi-Central Datasets. , 2018, 59, 1897.		19
103	Detection of Longitudinal Visual Field Progression in Glaucoma Using Machine Learning. American Journal of Ophthalmology, 2018, 193, 71-79.	1.7	84
104	The usefulness of CorvisST Tonometry and the Ocular Response Analyzer to assess the progression of glaucoma. Scientific Reports, 2017, 7, 40798.	1.6	30
105	Investigating the usefulness of a cluster-based trend analysis to detect visual field progression in patients with open-angle glaucoma. British Journal of Ophthalmology, 2017, 101, 1658-1665.	2.1	24
106	Effects of ocular and systemic factors on the progression of glaucomatous visual field damage in various sectors. British Journal of Ophthalmology, 2017, 101, 1071-1075.	2.1	9
107	The relationship between retinal nerve fibre layer thickness profiles and CorvisST tonometry measured biomechanical properties in young healthy subjects. Scientific Reports, 2017, 7, 414.	1.6	6
108	Applying "Lasso―Regression to Predict Future Glaucomatous Visual Field Progression in the Central 10 Degrees. Journal of Glaucoma, 2017, 26, 113-118.	0.8	11

#	Article	IF	CITATIONS
109	Validating the Usefulness of the "Random Forests―Classifier to Diagnose Early Glaucoma With Optical Coherence Tomography. American Journal of Ophthalmology, 2017, 174, 95-103.	1.7	42
110	The association between visual function and retinal structure in chronic central serous chorioretinopathy. Scientific Reports, 2017, 7, 16288.	1.6	16
111	The structure-function relationship measured with optical coherence tomography and a microperimeter with auto-tracking: the MP-3, in patients with retinitis pigmentosa. Scientific Reports, 2017, 7, 15766.	1.6	26
112	Using CorvisST tonometry to assess glaucoma progression. PLoS ONE, 2017, 12, e0176380.	1.1	8
113	Structural parameters associated with location of peaks of peripapillary retinal nerve fiber layer thickness in young healthy eyes. PLoS ONE, 2017, 12, e0177247.	1.1	11
114	Factors associated with the occurrence of a fall in subjects with primary open-angle glaucoma. BMC Ophthalmology, 2017, 17, 213.	0.6	3
115	Predicting Future Self-Reported Motor Vehicle Collisions in Subjects with Primary Open-Angle Glaucoma Using the Penalized Support Vector Machine Method. Translational Vision Science and Technology, 2017, 6, 14.	1.1	6
116	Association between Corneal Biomechanical Properties with Ocular Response Analyzer and Also CorvisST Tonometry, and Glaucomatous Visual Field Severity. Translational Vision Science and Technology, 2017, 6, 18.	1.1	17
117	Goldmann V Standard Automated Perimetry Underestimates Central Visual Sensitivity in Glaucomatous Eyes with Increased Axial Length. Translational Vision Science and Technology, 2017, 6, 13.	1.1	3
118	Cataract surgery causes biomechanical alterations to the eye detectable by Corvis ST tonometry. PLoS ONE, 2017, 12, e0171941.	1.1	18
119	The association between photoreceptor layer thickness measured by optical coherence tomography and visual sensitivity in glaucomatous eyes. PLoS ONE, 2017, 12, e0184064.	1.1	12
120	Evaluation of Glaucoma Progression in Large-Scale Clinical Data: The Japanese Archive of Multicentral Databases in Glaucoma (JAMDIG). , 2016, 57, 2012.		54
121	Assessing Visual Fields in Patients with Retinitis Pigmentosa Using a Novel Microperimeter with Eye Tracking: The MP-3. PLoS ONE, 2016, 11, e0166666.	1.1	34
122	The Relationship between Corvis ST Tonometry and Ocular Response Analyzer Measurements in Eyes with Glaucoma. PLoS ONE, 2016, 11, e0161742.	1.1	34
123	Risk Factors for Motor Vehicle Collisions in Patients with Primary Open-Angle Glaucoma: A Multicenter Prospective Cohort Study. PLoS ONE, 2016, 11, e0166943.	1.1	6
124	Detecting Preperimetric Glaucoma with Standard Automated Perimetry Using a Deep Learning Classifier. Ophthalmology, 2016, 123, 1974-1980.	2.5	189
125	The Usefulness of Gaze Tracking as an Index of Visual Field Reliability in Glaucoma Patients. , 2015, 56, 6233.		38
126	How Many Visual Fields Are Required to Precisely Predict Future Test Results in Glaucoma Patients When Using Different Trend Analyses?. , 2015, 56, 4076.		45

#	Article	IF	CITATIONS
127	Revalidating the Usefulness of a "Sector-Wise Regression―Approach to Predict Glaucomatous Visual Function Progression. , 2015, 56, 4332.		13
128	Estimating the Usefulness of Humphrey Perimetry Gaze Tracking for Evaluating Structure–Function Relationship in Glaucoma. , 2015, 56, 7801.		21
129	Applying "Lasso―Regression to Predict Future Visual Field Progression in Glaucoma Patients. , 2015, 56, 2334.		44
130	Investigating the Influence of Visual Function and Systemic Risk Factors on Falls and Injurious Falls in Glaucoma Using the Structural Equation Modeling. PLoS ONE, 2015, 10, e0129316.	1.1	22
131	Glaucomatous Visual Field Defect Severity and the Prevalence of Motor Vehicle Collisions in Japanese: A Hospital/Clinic-Based Cross-Sectional Study. Journal of Ophthalmology, 2015, 2015, 1-8.	0.6	17
132	The Relationship between Corvis ST Tonometry Measured Corneal Parameters and Intraocular Pressure, Corneal Thickness and Corneal Curvature. PLoS ONE, 2015, 10, e0140385.	1.1	54
133	A New Approach to Measure Visual Field Progression in Glaucoma Patients Using Variational Bayes Linear Regression. Investigative Ophthalmology and Visual Science, 2014, 55, 8386-8392.	3.3	45
134	Mapping Glaucoma Patients' 30-2 and 10-2 Visual Fields Reveals Clusters of Test Points Damaged in the 10-2 Grid That Are Not Sampled in the Sparse 30-2 Grid. PLoS ONE, 2014, 9, e98525.	1.1	33
135	Discriminating between Glaucoma and Normal Eyes Using Optical Coherence Tomography and the †Random Forests' Classifier. PLoS ONE, 2014, 9, e106117.	1.1	28
136	Combining Multiple HRT Parameters Using the †Random Forests' Method Improves the Diagnostic Accuracy of Glaucoma in Emmetropic and Highly Myopic Eyes. , 2014, 55, 2482.		7
137	Clustering Visual Field Test Points Based on Rates of Progression to Improve the Prediction of Future Damage. , 2014, 55, 7681.		24
138	Evaluation of various machine learning methods to predict vision-related quality of life from visual field data and visual acuity in patients with glaucoma. British Journal of Ophthalmology, 2014, 98, 1230-1235.	2.1	22
139	An Objective Evaluation of Gaze Tracking in Humphrey Perimetry and the Relation With the Reproducibility of Visual Fields: A Pilot Study in Glaucoma. Investigative Ophthalmology and Visual Science, 2014, 55, 8149-8152.	3.3	39
140	Impact of better and worse eye damage on quality of life in advanced glaucoma. Scientific Reports, 2014, 4, 4144.	1.6	20
141	The Relationship between Central Visual Field Damage and Motor Vehicle Collisions in Primary Open-Angle Glaucoma Patients. PLoS ONE, 2014, 9, e115572.	1.1	21
142	Five-year forecasts of the Visual Field Index (VFI) with binocular and monocular visual fields. Graefe's Archive for Clinical and Experimental Ophthalmology, 2013, 251, 1335-1341.	1.0	9
143	The relationship between visual acuity and central visual field sensitivity in advanced glaucoma. British Journal of Ophthalmology, 2013, 97, 1355-1356.	2.1	22
144	Quantitative Prediction of Glaucomatous Visual Field Loss from Few Measurements. , 2013, , .		6

#	Article	IF	CITATIONS
145	Relationship Between Position of Peak Retinal Nerve Fiber Layer Thickness and Retinal Arteries on Sectoral Retinal Nerve Fiber Layer Thickness. , 2013, 54, 5481.		75
146	Measuring Visual Field Progression in the Central 10 Degrees Using Additional Information from Central 24 Degrees Visual Fields and â€ĩLasso Regression'. PLoS ONE, 2013, 8, e72199.	1.1	20
147	Detection of Progression of Claucomatous Visual Field Damage Using the Point-Wise Method with the Binomial Test. PLoS ONE, 2013, 8, e78630.	1.1	16
148	The Influence of Intersubject Variability in Ocular Anatomical Variables on the Mapping of Retinal Locations to the Retinal Nerve Fiber Layer and Optic Nerve Head. , 2013, 54, 6074.		67
149	Identifying Areas of the Visual Field Important for Quality of Life in Patients with Glaucoma. PLoS ONE, 2013, 8, e58695.	1.1	88
150	A Novel Distribution of Visual Field Test Points to Improve the Correlation between Structure–Function Measurements. , 2012, 53, 8396.		24
151	Predicting retinal sensitivity using optical coherence tomography parameters in central serous chorioretinopathy. Graefe's Archive for Clinical and Experimental Ophthalmology, 0, , .	1.0	0